

Dynamic Analysis and Simulation of Astrojax

Lizhang Chen, Xianjue Bai, Jiaqi Xin and Yingli Niu*

School of Science, Beijing Jiaotong University, Beijing 100044, China; lzchen@bjtu.edu.cn (L.C.); xjbai@bjtu.edu.cn (X.B.); jqxin@bjtu.edu.cn (J.X.)

* Correspondence: ylniu@bjtu.edu.cn (Y.N.)

Abstract: Astrojax, also known as "Space Yo-Yo", is a toy popular throughout the United States[4]. Its structure is similar to a double pendulum, but there are obvious differences: the middle ball can slide along the rope. At present, the international research on the double pendulum is relatively mature and the simulation is diverse, but the research on the simulation and the steady-state of Astrojax is almost blank. This article focuses on the Astrojax horizontal orbit stable state and simulation algorithm. Our simulation model is developed based on Unity3D. We use C# to build the physical model behind it. The program uses three different algorithms: the explicit Euler algorithm, the Leapfrog algorithm, and the fourth-order Runge-Kutta algorithm to evolve the movement and obtains simulation results that are consistent with reality. The energy stability and effective running time of the three algorithms are compared. We also release applications for the windows platform and the Android platform.

Keywords: Astrojax; Stability state; Molecular Dynamics Integral; Stable Forced Vibration

1. Introduction

Astrojax is a toy popular throughout the United States[4]. Pass the rope through a ball with a hole so that the ball can move freely along the rope and tie another ball to one end of the rope. When you move the free end of the rope periodically, you can observe the complex movement of the two balls. This system is different from a double pendulum—the ball in the middle can slide freely along the rope. Because its motion resembles a planet, it is named Astrojax[5].

Citation: Lastname, F.; Lastname, F.; Lastname, F. Title. *Symmetry* **2021**, *1*, 0. <https://doi.org/>

Received:

Accepted:

Published:

Publisher's Note: MDPI stays neutral with regard to jurisdictional claims in published maps and institutional affiliations.

Copyright: © 2021 by the authors. Submitted to *Symmetry* for possible open access publication under the terms and conditions of the Creative Commons Attribution (CC BY) license (<https://creativecommons.org/licenses/by/4.0/>).

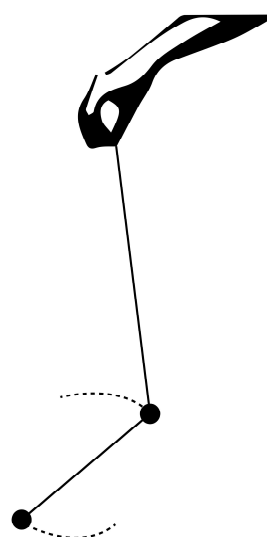


Figure 1. The Astrojax

20 Astrojax is full of educational significance. And it has been used to teach physics at
21 the grade school, high school, and college levels. NASA has taken Astrojax into outer
22 space as part of its "Toys in Space" education program[6].



Figure 2. NASA showed off the Astrojax movement under no gravity at the space station.[6]

23 Astrojax is a nonlinear system, for this dissipative system, air friction is the main
24 dissipation. When the periodic drive satisfies a certain pattern, the input power is equal
25 to the output power, and the ball will move in a certain stable pattern. At present, the
26 research on the double pendulum mainly focuses on the chaos and complexity of the
27 system[2], but the research on the simulation and steady state of the Astrojax is almost
28 blank. In this paper, we analyse the forces acting on Astrojax. Then we get the initial
29 conditions that can make the system stable without damping and drive. After that,
30 we use different algorithms to simulate Astrojax and present the energy changes with
31 iterations.

32 2. Dynamic Analysis of Horizontal Stable Orbit

33 Astrojax is a kind of complicated double pendulum ball motion, and the steady-
34 state of the horizontal orbit is the most easily formed stable-state in the experiment[1–3].
35 To solve the horizontal stable orbit mathematically, we first start with the undamped
36 horizontal stable state, establish a physical model to analyze the distribution of the
37 kinetic energy, potential energy, and total energy with the vertical angle and rotation
38 speed, and the transformation of the total energy with the vertical opening angle of
39 the rope. Finally, analyze the steady-state with damping which is closer to the actual
40 situation.

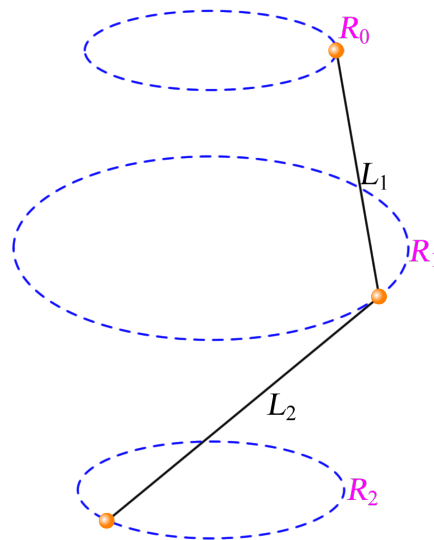


Figure 3. One of the stable movement–Horizontal Stable Orbit.

41 2.1. Dynamic Analysis of Undamped Steady State of Horizontal Orbit

42 First, let's take a look at its undamped movement on a horizontal orbit. This is one
 43 of the simplest ways to play Astrojax, and it is also the simplest stable state. Solving this
 44 state will be the basis for subsequent damping operation analysis.

45 2.1.1. Mathematical Model Establishment

46 In this state of motion, there is a small ball with a mass of m_0 at the top end, the
 47 mass of the small ball that can slide along the rope in the middle is m_1 , and the mass of
 48 the bottom ball is m_2 , which follows the top ball in a circular motion.

49 Most importantly, since there is no damping, all three balls are moving in the same
 50 plane, which will greatly simplify the difficulty of the problem, as shown in the figure
 51 on the bottom.

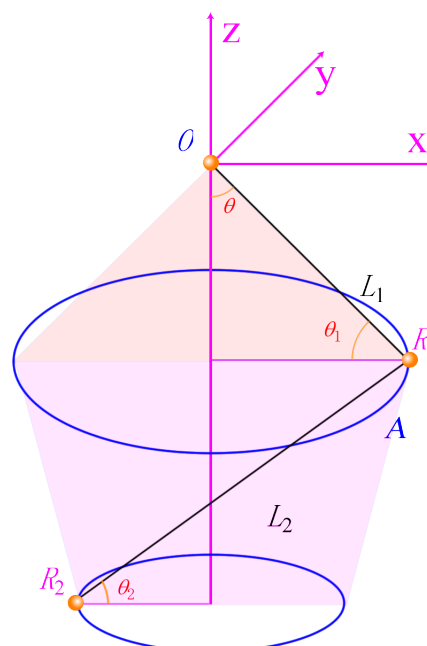


Figure 4. Undamped horizontally stable orbit.

2.1.2. Equation Establishment and Solution

It can be found that there are a total of six unknown parameters of the undamped steady state of horizontal orbit.

Table 1. Six Unknown parameters to describe the undamped steady state of horizontal orbit.

| Symbol | Physical Quantity |
|--------------|--|
| T : | cycle of circular motion |
| ω : | angular velocity of circular motion |
| θ_1 : | the angle between the upper two balls and the vertical direction |
| θ_2 : | the lower two balls and the vertical The angle of the direction |
| l_1 : | the length of the first section of rope |
| l_2 : | the length of the second half of the rope |

There are six unknown parameters of this system, but only five constraint equations as below. Especially, the steady-state of the system in this scenario is determined by the given parameter chosen from Table. 1.

$$T \cos \theta_1 = m_1 g + T \cos \theta_2 \quad (1)$$

$$T \sin \theta_1 + T \sin \theta_2 = m_1 \omega^2 l_1 \sin \theta_1 \quad (2)$$

$$T \sin \theta_2 = m_2 \omega^2 (l_2 \sin \theta_2 - l_1 \sin \theta_1) \quad (3)$$

$$T \cos \theta_2 = m_2 g \quad (4)$$

$$l_1 + l_2 = l \quad (5)$$

$$l - l_0 = \frac{T}{K} \quad (6)$$

In this case, as long as we are given any one of the unknown parameters, the remaining unknown parameters are all solvable, so such a state of motion can be completely determined.

2.1.3. Equation Visualization

We take the vertical angle θ_1 as a given variable. Next, we visualize the above solution results. Analytical solutions are obtained through the above equations and visualized below.

Under the undamped state, the kinetic energy and potential energy of the system are increased along with θ_1 . The kinetic energy, elasticity energy, potential energy, and total energy of the system are changed with θ_1 . As the angle increases, the kinetic energy and total energy decrease firstly and then increase, while the potential energy continues to increase. This means that the center of gravity of the two balls rises as the angle increases.

Under the undamped state, the radii of the middle ball and the bottom ball are distributed along with θ_1 of the rope. The kinetic energy and potential energy distribution along with the angular velocity is similar to the variety with θ_1 .

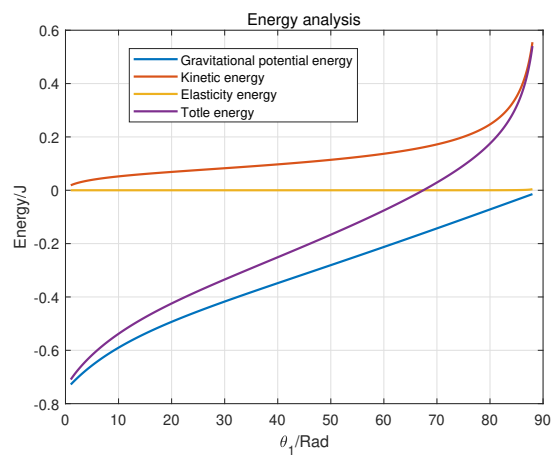


Figure 5. The kinetic energy, Elasticity energy, Potential energy, and Total energy of the system are changed with θ_1 .

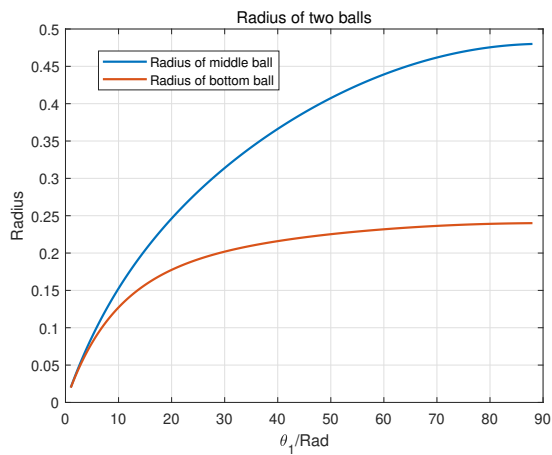


Figure 6. The Radius change of the Middle Ball and the Bottom Ball along with θ_1 .

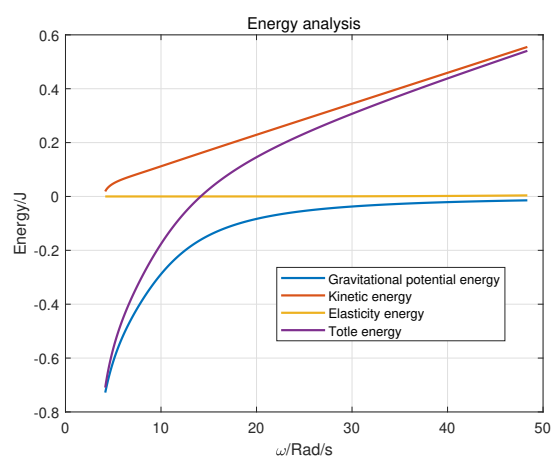


Figure 7. The kinetic energy and potential energy of the system are changed with the vertical opening angle.

2.2. Dynamic Analysis of Damped Steady State of Horizontal Orbit

Compare to the undamped state, the balls are dragged by air resistance in the case of damping. At this time, if three balls maintain a stable state still, they are not in the same plane. The ropes tied to the m_1 ball and the m_2 ball are dragged and formed

a horizontal angle ϕ_1 and ϕ_2 , so that the rope divides a part of the tension along the direction of movement. The air resistance is balanced and the stable state continues.

2.2.1. Mathematical Model Establishment

Consider the three small balls as three mass points, mark the middle ball as A , the upper ball as B , and the bottom ball as C , and suppose they rotate counterclockwise in the space. Establish the spatial rectangular coordinate system as shown in the figure. The spatial rectangular coordinate system here is left-handed.

Select the center of the circular motion of the top ball as the origin of the spatial rectangular coordinate system. The horizontal right is the x axis, the horizontal backward z axis, and the vertical upward y axis to establish a left-handed coordinate system. Diagram is showed below.

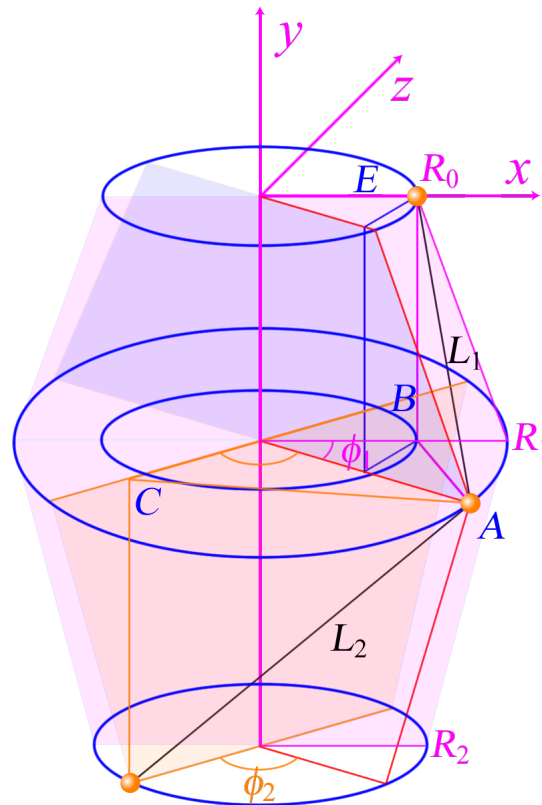


Figure 8. Damped horizontally stable orbit. All of the three balls moves with the same angular velocity

2.2.2. Equation Setting

Based on the left-hand coordinate system, the unit vectors in the three directions of xyz are :

$$\vec{x} = (1, 0, 0)'$$

$$\vec{y} = (0, 1, 0)'$$

$$\vec{z} = (0, 0, 1)'$$

It can be assumed that the radius of the top ball is R_0 , the radius of the middle ball is R_1 , the radius of the bottom ball is R_2 , the rope length between the top ball and the middle ball is L_1 , and the rope length between the middle ball and the bottom ball is L_2 . The position of the first ball is projected to the plane of the circular motion of the second ball, then the angle between the two lines is recorded as ϕ_1 , which is the phase difference corresponding to the circular motion of the two balls. The second ball is projected to the

bottom ball, and the phase difference between these two balls is recorded as ϕ_2 , in It is
to get the corresponding coordinate positions of the three balls B , A and C .

$$B : ((R_0 \cos(\omega t)), 0, R_0 \sin(\omega t)) \quad (7)$$

$$A : (R_1 \cos(\omega t - \phi_1), -h_1, R_0 \sin(\omega t - \phi_1)) \quad (8)$$

$$C : ((R_2 \cos(\omega t - \phi_1 - \phi_2), -h_1 - h_2, R_0 \sin(\omega t - \phi_1 - \phi_2)) \quad (9)$$

From this, the coordinate representation of the \vec{AB} and \vec{CA} vectors can be obtained,
and therefore the coordinate representation of the corresponding unit vector can be
obtained.

$$\vec{AB} = (R_0 \cos(\omega t) - R_1 \cos(\omega t - \phi_1), h_1, R_0 \sin(\omega t) - R_0 \sin(\omega t - \phi_1)) \quad (10)$$

$$\vec{CA} = (R_1 \cos(\omega t - \phi_1) - R_2 \cos(\omega t - \phi_1 - \phi_2), h_2, R_0 \sin(\omega t - \phi_1) - R_0 \sin(\omega t - \phi_1 - \phi_2)) \quad (11)$$

$$\vec{e}_1 = \frac{\vec{AB}}{|\vec{AB}|} \quad (12)$$

$$\vec{e}_2 = \frac{\vec{CA}}{|\vec{CA}|} \quad (13)$$

Look down from top to bottom to get the corresponding plane projection,

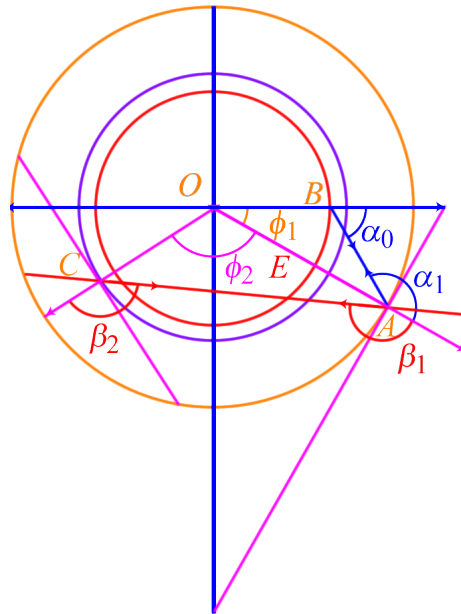


Figure 9. Horizontal projection of rectangular coordinate system of damped horizontal orbit

In this case, the problem is simplified to a circular motion in a plane. Such a motion
has to be mentioned as the most common circular motion. The method to deal with
the problem is to decompose \vec{A} and \vec{C} into the corresponding tangential acceleration
and the corresponding axial acceleration, and you can. Thus, the unit vector of the
corresponding direction is obtained.

$$\vec{A}_\perp = (-R_1 \cos(\omega t - \phi_1), 0, -R_1 \sin(\omega t - \phi_1)) \quad (14)$$

$$\vec{C}_\perp = (-R_2 \cos(\omega t - \phi_1 - \phi_2), 0, -R_2 \sin(\omega t - \phi_1 - \phi_2)) \quad (15)$$

$$e_{\vec{A}\perp} = \frac{\vec{A}_{\perp}}{|\vec{A}_{\perp}|} \quad (16)$$

$$e_{\vec{C}\perp} = \frac{\vec{C}_{\perp}}{|\vec{C}_{\perp}|} \quad (17)$$

$$\vec{A}_{\parallel} = (-R_1\omega \sin(\omega t - \phi_1), 0, R_1\omega \cos(\omega t - \phi_1)) \quad (18)$$

$$\vec{C}_{\parallel} = (-R_2\omega \sin(\omega t - \phi_1 - \phi_2), 0, -R_2\omega \cos(\omega t - \phi_1 - \phi_2)) \quad (19)$$

$$e_{\vec{A}\parallel} = \frac{\vec{A}_{\parallel}}{|\vec{A}_{\parallel}|} \quad (20)$$

$$e_{\vec{C}\parallel} = \frac{\vec{C}_{\parallel}}{|\vec{C}_{\parallel}|} \quad (21)$$

At the same time, for the middle ball, it is assumed that it is not subject to the friction of the rope, and the resistance to the rope is ignored. Then, the middle ball can be simplified as a moving pulley. In this case, the two ends of the rope can be approximately treated as equal rope tension at both ends. Therefore, the middle and bottom balls are regarded as a whole, and the upper half of the rope is projected. In the vertical direction, this force component should be balanced with the gravity of the small ball in the middle and bottom.

Similarly, when this section of rope is projected into the horizontal plane, this component force can be used as the axial force of the latter two balls to make circular motions, driving the middle and bottom balls to make circular motions. In the same way, do the same projection process for the second half of the rope, and you can get the force analysis of the bottom ball. So we got the six equations

$$T\vec{e}_1 \cdot \vec{y} = (m_1 + m_2)g \quad (22)$$

$$T\vec{e}_2 \cdot \vec{y} = m_2g \quad (23)$$

$$T\vec{e}_1 \cdot e_{\vec{A}\perp} - T\vec{e}_2 \cdot e_{\vec{A}\perp} = \omega^2 m_1 R_1 \quad (24)$$

$$T\vec{e}_1 \cdot e_{\vec{A}\parallel} - T\vec{e}_2 \cdot e_{\vec{A}\parallel} = \eta\omega R_1 \quad (25)$$

$$T\vec{e}_2 \cdot e_{\vec{C}\parallel} = \eta\omega R_2 \quad (26)$$

$$T\vec{e}_2 \cdot e_{\vec{C}\perp} = \omega^2 m_2 R_2 \quad (27)$$

3. Equation Solving

Now we have these six equations for the Astrojax system with damping and driving. By simplifying, the above six equations can be transferred into the following three equations (a1), (a2) and (a3). And we will find the numerical solutions equations in this part.

3.1. Up to down order calculation

1) Length constraint

$$L_1^2 = R_0^2 + R_1^2 - 2R_0R_1 \cos \phi_1 + H_1^2 \quad (a1)$$

2) Force direction constraint

$$\frac{T_{01y}}{\sqrt{T_{01\parallel}^2 + T_{01\perp}^2}} = \frac{H_1}{\sqrt{R_0^2 + R_1^2 - 2R_0R_1 \cos \phi_1}} \quad (a2)$$

where T_{01y} indicates the projection of the rope tension in the vertical direction, $T_{01\parallel}$ indicates the projection of the rope tension in the horizontal direction and $T_{01\perp}$ indicates the projection of the rope tension in the vertical direction.
 3) Force direction constraint

$$\frac{T_{01\parallel}}{T_{01\perp}} = \tan(\pi - \alpha_1) = \frac{\sin \phi_1}{\frac{R_1}{R_0} - \cos \phi_1} \quad (\text{a3})$$

Define

$$\frac{T_{01\parallel}}{T_{01\perp}} \equiv \sigma \quad (\text{a4})$$

and

$$\frac{T_{01y}}{\sqrt{T_{01\parallel}^2 + T_{01\perp}^2}} \equiv \frac{\kappa}{r} \quad (\text{a5})$$

where

$$\sigma \equiv \frac{\eta}{m_1 \omega} \quad (\text{a6})$$

$$\xi \equiv \frac{g}{\omega^2 R_0} \quad (\text{a7})$$

$$\kappa \equiv \frac{\xi}{\sqrt{\sigma^2 + 1}} \quad (\text{a8})$$

and

$$r \equiv \frac{R_1}{R_0} \quad (\text{a9})$$

$$h \equiv \frac{H_1}{R_0} \quad (\text{a10})$$

$$l \equiv \frac{L_1}{R_0} \quad (\text{a11})$$

Then for the equations

$$r^2 - 2r \cos \phi_1 + 1 + h^2 - l^2 = 0 \quad (\text{a12})$$

$$\kappa \sqrt{1 + r^2 - 2r \cos \phi_1} = hr \quad (\text{a13})$$

$$\sigma r - \sigma \cos \phi_1 - \sin \phi_1 = 0 \quad (\text{a14})$$

We have

$$h = \frac{\kappa l}{\sqrt{r^2 + \kappa^2}} \quad (\text{a15})$$

$$\cos \phi_1 = \frac{r^4 + r^2(\kappa^2 - l^2 + 1) + \kappa^2}{2r(r^2 + \kappa^2)} \quad (\text{a16})$$

Insert Eq. (a16) into Eq. (a14)

$$r^8 + 2\left(l^2 \frac{\sigma^2 - 1}{\sigma^2 + 1} + (\kappa^2 - 1)\right)r^6 + \left[(\kappa^2 - 2)^2 + (l^2 - 1)^2 - 4 + 2\kappa^2 l^2 \frac{\sigma^2 - 1}{\sigma^2 + 1}\right]r^4 - 2\kappa^2(l^2 + \kappa^2 - 1)r^2 + \kappa^4 = 0 \quad (\text{a17})$$

140 Set $r^2 = x$, then Eq. (a17) becomes

$$x^4 + 2\left(l^2 \frac{\sigma^2 - 1}{\sigma^2 + 1} + \kappa^2 - 1\right)x^3 + \left[(\kappa^2 - 2)^2 + (l^2 - 1)^2 - 4 + 2\kappa^2 l^2 \frac{\sigma^2 - 1}{\sigma^2 + 1}\right]x^2 - 2\kappa^2(l^2 + \kappa^2 - 1)x + \kappa^4 = 0 \quad (\text{a18})$$

141 which can be solved numerically. Hence, we can have the value of R_1 after solving Eq.
 142 (a18) given R_0, ω . Note that $0 < L_1 < L_0$, so we can find the best value of L_1 that satisfies
 143 these three equations. Furthermore, we can have L_2 because we know the coefficient
 144 of elasticity of the rope. So we can repeat this process to calculate R_2 since we have
 145 obtained the value of R_1, ω and L_2 . After that, we can determine the position and the
 146 velocity of each ball. Note that, the order of this process is from the top ball to the bottom
 147 ball, which is intuitive. But we have to find solutions of the quartic equation(a18). So
 148 we will introduce the other calculation process, which can avoid calculating the quartic
 149 equation(a18).

150 3.2. Reverse order calculation (down to the up)

151 1) Length constraint

$$L_1^2 = R_0^2 + R_1^2 - 2R_0R_1 \cos \phi_1 + H_1^2 \quad (\text{b1})$$

152 2) Force direction constraint

$$\frac{T_{01y}}{\sqrt{T_{01\parallel}^2 + T_{01\perp}^2}} = \frac{H_1}{\sqrt{R_0^2 + R_1^2 - 2R_0R_1 \cos \phi_1}} \quad (\text{b2})$$

153 3) Force direction constraint

$$\frac{T_{01\parallel}}{T_{01\perp}} = \tan(\pi - \alpha_1) = \frac{\sin \phi_1}{\frac{R_1}{R_0} - \cos \phi_1} \quad (\text{b3})$$

154 Define

$$T_{01\parallel} = \eta\omega R_1 - T_{02\parallel} \quad (\text{b4})$$

$$T_{01\perp} = m_1\omega^2 R_1 - T_{02\perp} \quad (\text{b5})$$

155 and

$$\frac{m_1 g}{\sqrt{(\eta\omega R_1 - T_{02\parallel})^2 + (m_1\omega^2 R_1 - T_{02\perp})^2}} \equiv \kappa \quad (\text{b6})$$

156 where

$$\sigma \equiv \frac{\eta\omega R_1 - T_{02\parallel}}{m_1\omega^2 R_1 - T_{02\perp}} \quad (\text{b7})$$

157 and

$$r \equiv \frac{R_0}{R_1} \quad (\text{b8})$$

$$h \equiv \frac{H_1}{R_1} \quad (\text{b9})$$

$$l \equiv \frac{L_1}{R_1} \quad (\text{b10})$$

158 Then for the equations

$$r^2 + 1 - 2r \cos \phi_1 + h^2 - l^2 = 0 \quad (\text{b11})$$

$$\kappa \sqrt{1 + r^2 - 2r \cos \phi_1} = h \quad (\text{b12})$$

$$\sigma r^{-1} - \sigma \cos \phi_1 - \sin \phi_1 = 0 \quad (\text{b13})$$

159 We have

$$h = \frac{\kappa l}{\sqrt{1 + \kappa^2}} \quad (\text{b14})$$

$$\cos \phi_1 = \frac{1}{2r} \left(r^2 + 1 - \frac{l^2}{\kappa^2 + 1} \right) \quad (\text{b15})$$

160 Insert Eq. (b15) into Eq. (b13)

$$(\kappa^2 + 1)r^4 - 2(\kappa^2 + l^2 + 1)r^2 + 2l^2 \frac{\sigma^2 - 1}{\sigma^2 + 1} + \frac{l^4}{\kappa^2 + 1} + \kappa^2 + 1 = 0 \quad (\text{b16})$$

161 Set $r^2 = x$, then Eq. (b16) becomes

$$(\kappa^2 + 1)x^2 - 2(\kappa^2 + l^2 + 1)x + 2l^2 \frac{\sigma^2 - 1}{\sigma^2 + 1} + \frac{l^4}{\kappa^2 + 1} + \kappa^2 + 1 = 0 \quad (\text{b17})$$

162 which has root formula. Compared with the previous calculation order, the reverse
163 calculation order can avoid solving quartic equation and the final equation has root
164 formula.

165 4. Simulation Algorithm Analysis

166 After analyzing the dynamic characteristics of Astrojax, we used three different
167 dynamic integration methods to establish the simulation model, and realized the vi-
168 sualization of the simulation model to verify the horizontal orbit motion mode in the
169 dynamic analysis research. At the same time, three indicators are used to judge the
170 performance of each algorithm, namely the operating speed S , the stability of the energy
171 E_{std} , and the stability of the orbit R_{std} . The calculation methods of the three indicators
172 are as follows:

$$S = \frac{Time}{10w\ Steps} \quad (28)$$

$$E_{std} = \frac{\sum_{i=1}^n (E_i - E_0)^2}{n - 1} \quad (29)$$

$$Error = |R_{ana}^{\vec{}} - R_{sim}^{\vec{}}| \quad (30)$$

$$R_{std} = \sqrt{\frac{\sum_{i=1}^n (Error_i)^2}{n - 1}} \quad (31)$$

173 4.1. Introduction to Three Algorithms

174 Three algorithms of molecular dynamics integration: The explicit Euler algorithm,
175 the Leapfrog algorithm, and the fourth-order Runge-Kutta Algorithm. Leapfrog method
176 has good integration accuracy and low algorithm complexity.

177 4.1.1. The Explicit Euler Algorithm

178 The Explicit Euler method is a first-order numerical method. It is the most basic type
179 of explicit method for solving numerical ordinary differential equations. The explicit
180 Euler method has the following form:

$$y_{n+1} = y_n + hf(y_n, t_n) \quad (32)$$

181 In our astrojax project, we know the speed and displacement of the balls, $v(t)$ $x(t)$,
182 we can calculate the acceleration, a . Then we use the Euler method:

$$v(t + \Delta t) = v(t) + a\Delta t \quad (33)$$

$$x(t + \Delta t) = x(t) + v(t + \Delta t)\Delta t \quad (34)$$

183 to get the speed and displacement of the next step.

184 4.1.2. The Leapfrog Algorithm

185 Leapfrog method is divided into three steps, the steps are as follows:

186 First jump: The starting point of the integration is the first jump at the coordinate
187 $x(t)$ at time t and the speed $v(t - \frac{1}{2}\delta t)$ at $(t - \frac{1}{2}\delta t)$ time ; the frog (the iterated parameter)
188 first stands at the position of $x(t)$ and calculates it according to the coordinates When
189 the particle is forced, the acceleration $a(t)$ at time t is naturally derived to complete the
190 first jump.

191 Second jump: Calculate the speed at time $t + \frac{1}{2}\delta t$ according to $a(t)$. Based on
192 $v(t + \frac{1}{2}\delta t) = v(t - \frac{1}{2}\delta t) + a(t)\delta t$, finishes the second jump.

193 Third jump: Calculate the position at time t based on the speed at $t + \frac{1}{2}\delta t$. Based on
194 $x(t + \frac{1}{2}\delta t) = x(t - \frac{1}{2}\delta t) + v(t)\delta t$, the third jump is completed. The speed at time t can
195 be the average of the speed at time $t - \frac{1}{2}\delta t$ and $t + \frac{1}{2}\delta t$.

196 4.1.3. The fourth-order Runge-Kutta Algorithm

197 The Runge-Kutta method is an important type of implicit or explicit iterative
198 method for the solution of nonlinear ordinary differential equations. Due to the high
199 accuracy of this algorithm, measures are taken to suppress errors, so its implementation
200 principle is also more complicated. The formula is as follows:

$$y_{n+1} = y_n + \frac{h}{6}(k_1 + 2K_2 + 2K_3 + K_4) \quad (35)$$

$$k_1 = f(y_n + t_n) \quad (36)$$

$$k_2 = f(y_n + \frac{hk_1}{2}, t_n + \frac{h}{2}) \quad (37)$$

$$k_3 = f(y_n + \frac{hk_2}{2}, t_n + \frac{h}{2}) \quad (38)$$

$$k_4 = f(y_n + hk_3, t_n + h) \quad (39)$$

201 We denote the position and velocity of the ball as $x(t)$, $v(t)$, calculate their respective
202 forces to get the acceleration, we call this a_1 . The iteration equations are as follow:

$$a_1 = a_1\Delta t \quad (40)$$

$$v_1 = v_1\Delta t \quad (41)$$

203 In the next step, we take:

$$x_2 = x(t) + \frac{v_1}{2} \quad (42)$$

$$v_2 = v(t) + \frac{a_1}{2} \quad (43)$$

Further calculations get another acceleration, we call this a_2 . In the same way we get a_3, a_4, v_3, v_4 . Finally, the x and v in the next step can be expressed as:

$$v(t + \Delta t) = \Delta t \frac{a_1 + 2a_2 + 2a_3 + a_4}{6} + v(t) \quad (44)$$

$$x(t + \Delta t) = \Delta t \frac{v_1 + 2v_2 + 2v_3 + v_4}{6} + x(t) \quad (45)$$

4.2. Specific Analysis of Simulation Algorithm

In the experiment, we noticed two unexpected situations, namely: two balls collision and rope slack.

1. The situation where two balls collide; We adopt the strategy commonly used in numerical simulation, considering the larger elastic coefficient of the ball; the two balls have a small deformation during the collision, so the collision is regarded as a completely elastic collision.

2. The slack of the rope: During exercise, the rope will stretch to a certain extent. The force on the two balls is calculated according to the elongation and the stiffness coefficient; when the rope length is loose, the rope tension is zero.

4.3. Equation Establishment

n : represents the n th time point; P : the position of the top ball; A : the position of the middle ball; B : The position of the end ball; k : The stiffness coefficient measured by the experiment, the elasticity of the rope.

$$\overrightarrow{P_n A_n} = \overrightarrow{O A_n} - \overrightarrow{O P_n} \quad (46)$$

$$\overrightarrow{A_n B_n} = \overrightarrow{O B_n} - \overrightarrow{O A_n} \quad (47)$$

$$\vec{e}_1 = \frac{\overrightarrow{P_n A_n}}{|\overrightarrow{P_n A_n}|} \quad (48)$$

$$\vec{e}_2 = \frac{\overrightarrow{A_n B_n}}{|\overrightarrow{A_n B_n}|} \quad (49)$$

$$\Delta L_n = |\overrightarrow{P_n A_n}| + |\overrightarrow{A_n B_n}| - L_0 \quad (50)$$

$$f_0 = k \cdot \Delta L_n \quad (51)$$

$$\vec{f}_{A_n} = -f_0 \vec{e}_1 + f_0 \vec{e}_2 - \vec{G}_{A_{n-1}} \quad (52)$$

$$\vec{f}_{B_n} = -f_0 \vec{e}_2 - \vec{G}_{B_{n-1}} \quad (53)$$

4.4. Three dynamics integral algorithms comparison

After the dynamic analysis and the simulation algorithm establishment of both undamped and damped condition with horizontal orbit, a series of simulation experiments are took to verify the validity of mathematical analysis, and to compare the best algorithm.

First, carry out the simulation experiment without damping, and select $m = 31.88(g)$ respectively $l_0 = 1.2(m)$ and $m = 29.96(g)$ respectively $l_0 = 1.13(m)$ two sets of initial conditions, under each condition, five different stable states are selected, which are $\theta_0 = 1^\circ, 23^\circ, 45^\circ, 67^\circ, 89^\circ$, each steady state is calculated three times to calculate the average running time. The results are as follows:

| Expriment Data(Undamped Condition) | | | | |
|------------------------------------|----------------|------------------|------------------------|------------------------|
| Initial Parameters | Algorithm | Calculate Time/s | R_{std} | E_{std} |
| m=31.88(g) L0=1.2(m) | Explicit Euler | 0.674 | 3.208×10^{-4} | 3.965×10^{-6} |
| | Leapfrog | 1.209 | 3.811×10^{-5} | 3.904×10^{-6} |
| | RK4 | 2.433 | 3.809×10^{-5} | 4.911×10^{-6} |
| m=29.96(g) L0=1.13(m) | Explicit Euler | 0.680 | 2.809×10^{-4} | 3.489×10^{-6} |
| | Leapfrog | 1.163 | 3.374×10^{-5} | 3.520×10^{-6} |
| | RK4 | 2.352 | 3.372×10^{-5} | 4.504×10^{-6} |

It can be seen that within the simulation time of 10 seconds, the three algorithms have good error performance in energy stability and orbital stability. The best performance of the three algorithms is the RK4 algorithm, which is obvious, because RK4 is a fourth-order algorithm, while explicit Euler is first-order, and leaffrog is second-order. So it is better to compare the error with time weighted.

$$R'_{std} = R_{std} \times Calculate\ Time$$

See as the table below:

| Undamped Condition with Time Weighted | | | |
|---------------------------------------|-----------------------|-----------------------|-----------------------|
| Algorithm | Explicit Euler | Leapfrog | RK4 |
| R'_{std} | 2.03×10^{-4} | 4.26×10^{-5} | 8.56×10^{-5} |
| E'_{std} | 2.52×10^{-6} | 4.40×10^{-6} | 1.12×10^{-5} |

It can be seen that after the time weighted, the second-order leapfrog algorithm is optimal in orbital error performance, and Explicit Euler algorithm makes the best performance.

Secondly, carry out the simulation experiment with damping, and still choose two sets of initial conditions. Under each condition, five different stable states are selected. The average simulation experiment data with time weighted are as follows:

| Damped Condition with Time Weighted | | | |
|-------------------------------------|-----------------------|-----------------------|-----------------------|
| Algorithm | Explicit Euler | Leapfrog | RK4 |
| R'_{std} | 2.17×10^{-3} | 9.31×10^{-4} | 2.11×10^{-4} |
| E'_{std} | 3.01×10^{-4} | 3.23×10^{-4} | 4.30×10^{-4} |

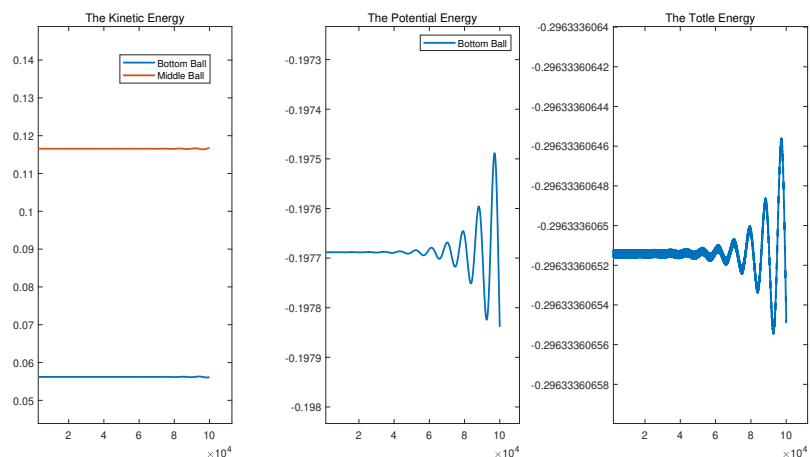


Figure 10. One of the energy performance in 10s under damped condition

5. Reference

1. Philip Du Toit, The Astrojax Pendulum and the N-Body Problem on the Sphere: A study in reduction, variational integration, and pattern evocation. **2005**, *10 Jun*, 1–28.
2. Andras Karsai, Steven Harrington, and Colin Campbell, The Astrojax Pendulum **2014**, *10 Dec*, 1–8.
3. Colin Campbell, Steven Harrington, and Andy Karsai, Variable Length Spherical Pendulum: the Astrojax.
4. Wikipedia. Available online: <https://en.wikipedia.org/wiki/Astrojax> (2021).
5. Astrajax. Available online: <https://astrojax.com> (2021).
6. NASA: International Toys in Space. Available online: <https://www.nasa.gov> (2021).

Acknowledgments: This project is supported by Beijing Jiaotong University Training Program of Innovation and Entrepreneurship for Undergraduates, Beijing Training Program of Innovation and Entrepreneurship for Undergraduates and National Training Program of Innovation and Entrepreneurship for Undergraduates.

Appendix A

We compared the motion trajectory obtained by the simulation with the experiment, and found that in a long period of time, our simulation model is in good agreement with the actual situation. With the help of a simulation program, many experiments can be moved to everyone's mobile phones. Also, virtual simulation can verify and demonstrate our theoretical analysis. Students can adjust the parameters themselves in the virtual simulation to explore more stable states.

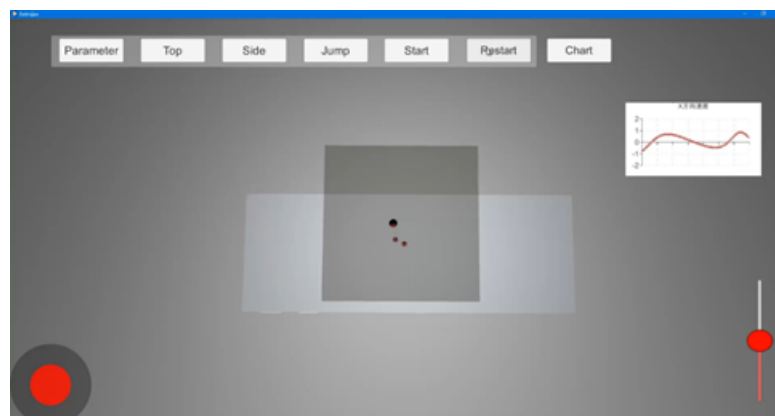


Figure A1. The display of our project in the windows operating platform

The picture shows our simulation program: the red button in the lower left corner is similar to the joystick when we play mobile games, which can control the horizontal movement of the top ball, while the red button in the bottom right corner can control the vertical movement of the top ball; We can choose to observe the motion state of the system from different perspectives; we can also import data and set the data conditions ourselves if we click the parameter button; the curve in the upper right corner represents the change of the speed of the end ball in the x direction over time. In addition, we can switch perspective if we click the top or side button (Figure A1. is from the top perspective; Figure A2. is from the side perspective).

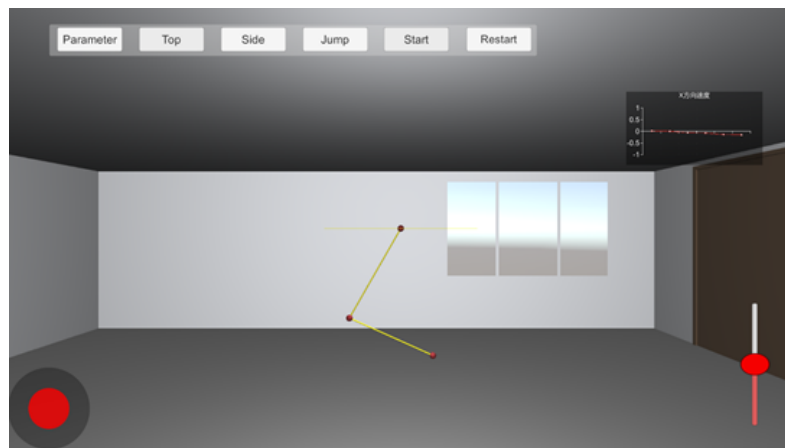


Figure A2. The display of our project in the windows operating platform